

# Mechanistic Studies of the Reduction of Nitroarenes by NaBH<sub>4</sub> or Hydrosilanes Catalyzed by Supported Gold Nanoparticles

Stella Fountoulaki,<sup>†</sup> Vassiliki Daikopoulou,<sup>†</sup> Petros L. Gkizis,<sup>†</sup> Ioannis Tamiolakis,<sup>‡</sup> Gerasimos S. Armatas,<sup>‡</sup> and Ioannis N. Lykakis<sup>\*†</sup>

<sup>†</sup>Department of Chemistry, Aristotle University of Thessaloniki, University Campus, 54124 Thessaloniki, Greece

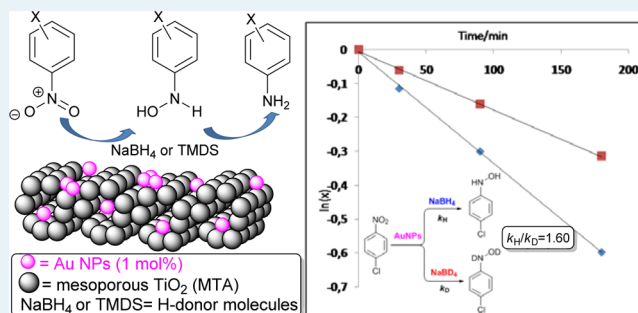
<sup>‡</sup>Department of Materials Science and Technology, University of Crete, University Campus, 71003 Voutes Heraklion, Crete, Greece

## Supporting Information

**ABSTRACT:** Herein, we show that mesoporous titania-supported gold nanoparticle assemblies (Au/MTA) catalyze the activation of NaBH<sub>4</sub> and 1,1,3,3-tetramethyl disiloxane (TMDS) compounds, which act as transfer hydrogenation agents for the reduction of nitroarenes to the corresponding anilines in moderate to high yields. On the other hand, nitroalkanes are reduced to the corresponding diazo and hydrazo compounds under the studied conditions. The substantial measured primary kinetic isotope effects found here suggested that B–H bond cleavage occurs in a rate-determining step and [Au]–H active hybrids are formed, which are responsible for the reduction of nitroarenes to the

corresponding amines. Formal Hammett-type kinetic analysis of a range of para-X-substituted nitroarenes lends support to this hypothesis. Nitro compounds substituted with electron-withdrawing groups were reduced faster than the corresponding compounds with electron-donating groups. The presence of water enhanced the catalytic activity of Au/MTA in aprotic solvents. Nuclear magnetic resonance studies support the formation of the corresponding hydroxylamines as the only intermediate products. On the basis of the high observed chemoselectivities and the fast and clean reaction processes, these catalytic systems, i.e., Au/MTA-NaBH<sub>4</sub> and Au/MTA-TMDS, show promise for the efficient synthesis of aromatic amines at industrial levels.

**KEYWORDS:** gold nanoparticles, heterogeneous catalysis, nitro compounds, selective reduction, kinetic isotope effects, Hammett kinetics



## 1. INTRODUCTION

Synthesis of anilines or amines from the corresponding nitro compounds is an important process in the laboratory and in the chemical industry because of their versatility in several biologically active natural products, dyes, and pharmaceuticals.<sup>1</sup> The most popular and promising route for the transformation of nitro groups to amine groups is transition metal-catalyzed hydrogenation,<sup>2</sup> although low chemoselectivities are observed, especially when other reducible groups are present. Therefore, the development of an efficient catalytic system for chemoselective reduction of nitro compounds is a challenging area. So far, supported gold nanoparticles (AuNPs),<sup>3–5</sup> such as Au/TiO<sub>2</sub>,<sup>4</sup> have been used successfully for the selective transformation of nitro groups into amines through a direct hydrogenation process, yet that process requires harsh reduction conditions, i.e., high temperatures and H<sub>2</sub> pressures. In addition, the reduction of nitroarenes in the presence of AuNPs and several reducing agents such as CO/H<sub>2</sub>O,<sup>6</sup> HCOONH<sub>4</sub>,<sup>7</sup> alcohols,<sup>8</sup> NaBH<sub>4</sub>,<sup>9</sup> hydrosilanes,<sup>10</sup> hydrazine,<sup>11</sup> and ammonia borane<sup>12</sup> has been studied. In a similar context, the activation of NaBH<sub>4</sub> by gold nanoparticles was mainly investigated in the chemoselective reduction of 4-nitrophenol to 4-aminophenol.<sup>9</sup>

Recently, we demonstrated mesoporous Au-loaded TiO<sub>2</sub> nanoparticle assemblies (Au/MTA) featuring controllable gold particle size (i.e., ranging from 3 to 10 nm) to be highly effective catalysts for the chemoselective reduction of nitroarenes into amines, using sodium borohydride as a reducing agent under ambient conditions.<sup>13</sup> The results suggested that Au/MTA associated with 5 nm Au particles is a uniquely active catalyst for such hydrogenation reactions, providing exceptionally high selectivity (>99%) and conversion yield (>90%) to the corresponding aryl amines. Following our interest in novel applications of supported AuNPs in several organic transformations,<sup>14</sup> we turned our focus on the mechanistic studies of the Au-mediated reduction of nitroarenes in the presence of borohydrides or hydrosilanes. Previous kinetic isotope effect studies under hydrogenation of nitroaromatics with Au/TiO<sub>2</sub> showed that the rate-determining step in this process is the dissociation of H<sub>2</sub> on gold particles.<sup>4d</sup> In addition, Cao and co-workers proposed that the Au/meso-CeO<sub>2</sub> catalyzes the controlled formation of reduced products, such as azoxy, azo,

Received: March 21, 2014

Revised: June 26, 2014

Published: August 25, 2014

and amine compounds, in the presence of 2-propanol under specific reaction conditions.<sup>8a</sup> Herein, we report a detailed mechanistic route for the AuNP-catalyzed reduction of nitroarenes in the presence of sodium borohydride or hydrosilane reductants. The catalytic results are interpreted on the basis of kinetic isotope effects (KIEs) and Hammett-type kinetic analysis, as well as on the product characterization by liquid chromatography–mass spectrometry (LC–MS) and nuclear magnetic resonance (NMR) spectroscopy.

## 2. EXPERIMENTAL DETAILS

**2.1. General.** The aromatic nitro compounds used as substrates were of high purity and commercially available from Aldrich. Primary nitroalkanes were synthesized via oxidation of the corresponding amines according to the literature procedure using excess *m*-CPBA.<sup>15</sup> Brij-58 surfactant [HO-(CH<sub>2</sub>CH<sub>2</sub>O)<sub>20</sub>C<sub>16</sub>H<sub>33</sub>; *M<sub>n</sub>* ~ 1124], titanium tetrachloride (99.9%), anatase TiO<sub>2</sub> (99.8%), HAuCl<sub>4</sub>, and absolute ethanol (99.8%) were purchased from Sigma-Aldrich. Titanium(IV) isopropoxide (>98%) was purchased from Merck. TiO<sub>2</sub> nanoparticles (P25) were purchased from Degussa AG.

**2.2. Preparation of Catalysts.** Catalysts Au/TiO<sub>2</sub>, Au/Al<sub>2</sub>O<sub>3</sub>, and Au/ZnO (~1 wt % in Au) used in this study are commercially available. The titania-supported gold catalysts Au/MTA were synthesized by the deposition–precipitation method over mesoporous TiO<sub>2</sub> nanoparticle assemblies (MTA),<sup>16</sup> according to the method described previously.<sup>13</sup> Briefly, an aqueous solution of Au(en)<sub>3</sub>Cl<sub>3</sub> (5 mL) corresponding to the desired gold loading was adjusted to pH 10 with a 1 M NaOH solution. Subsequently, 100 mg of MTA was dispersed into the gold solution with vigorous stirring for 1 h, and the resulting powder was recovered by filtration, washed with water, and dried at 40 °C under vacuum. Reduction of gold species on the surface of MTA was conducted by suspending (for 30 min at 25 °C) 100 mg of Au/MTA in 1.5 mL of a 0.3 M NaBH<sub>4</sub> ethanolic solution. The purple-colored solid was then recovered by filtration, washed with water and ethanol, and dried in a vacuum oven at 80 °C. A series of Au/MTA(*x*) catalysts with various Au loadings (*x* = 0.5, 1, and 2 wt %) were prepared by varying the amount of Au in the reaction mixture. For comparative studies, the Au/TiO<sub>2</sub> (P25) material was prepared via a procedure similar to that used for Au/MTA, but depositing 2 wt % gold on commercially available TiO<sub>2</sub> nanoparticles (Degussa P25).

**2.3. Physical Characterization.** Small-angle X-ray scattering (SAXS) measurements were performed on a JJ X-ray system (Denmark) equipped with a Rigaku Helium-3 detector and a Cu ( $\lambda = 1.54098 \text{ \AA}$ ) rotating anode operated at 40 kV and 40 mA. The sample-to-detector distance and the center of beam were precisely determined by calibration with the Ag-behenate (*d*<sub>001</sub> = 58.38 Å) standard. The average size of spherically shaped TiO<sub>2</sub> particles was determined from the scattering data, using the Guinier approximation:  $I(q) = A \exp(-q^2 R_g^2/3)$ , where *I* is the scattering intensity and *R<sub>g</sub>* is the radius of gyration. Nitrogen adsorption and desorption isotherms were measured at –196 °C using a Quantachrome NOVA 3200e volumetric analyzer. Before analysis, the samples were degassed at 130 °C under vacuum (<10<sup>–5</sup> Torr) for 12 h to remove the moisture. The specific surface area was calculated using the Brunauer–Emmett–Teller (BET) method on the adsorption data in the relative pressure (*P/P*<sub>0</sub>) range of 0.05–0.22. The total pore volumes were derived from the adsorbed volume at *P/P*<sub>0</sub> = 0.95, and the pore size distributions were calculated by the

nonlocal density functional (NLDFT) method on the basis of the adsorption data. Transmission electron microscopy (TEM) analysis was conducted using a JEOL JEM-2100 electron microscope (operating at an accelerating voltage of 200 kV). Elemental microprobe analysis was conducted on a JEOL JSM-6390LV scanning electron microscope (SEM) equipped with an Oxford INCA PantaFET-x3 energy dispersive X-ray spectroscopy (EDS) detector. Data were acquired at an accelerating voltage of 20 kV with an accumulation time of 60 s.

**2.4. Catalytic Reactions.** Supported gold catalyst Au/MTA or Au/TiO<sub>2</sub> (1 mol % Au) was placed in a 5 mL glass reactor, followed by the addition of ethanol (1 mL), nitro compound (0.1 mmol), and NaBH<sub>4</sub> (0.4–0.6 mmol) or TMDS (0.25 mmol), and the reaction mixture was stirred at room temperature for a selected time. The reaction was monitored by thin layer chromatography (TLC), and after completion, the slurry was filtered under pressure through a short pad of Celite and silica to withhold the catalyst with the aid of ethanol or methanol (~5 mL). The filtrate was evaporated under vacuum to afford the corresponding products in pure form. Product analysis was conducted by <sup>1</sup>H NMR and <sup>13</sup>C NMR spectroscopy (Bruker AM 300 and Agilent AM 500). Identification of the products was realized by comparing the NMR spectral data with those of the commercially available pure substances. Mass spectra were determined on an LC–MS-2010 EV instrument (Shimadzu) under electrospray ionization (ESI) conditions. Reusability testing of the catalyst was conducted in the case of the Au/MTA(2) sample through the hydrogenation of 4-nitrotoluene. A 2 mL mixture of the feeding solution (0.2 mmol of 4-nitrotoluene and 1 mmol of NaBH<sub>4</sub>) together with 20 mg of the catalyst (1 mol % Au) was placed into a vial. Each catalytic reaction was stopped after 2 h, and the catalyst was collected by filtration, washed with ethanol, and dried in an oven at 100 °C for 12 h. Then the recovered catalyst was used for the next catalytic run without any reactivation.

## 3. RESULTS AND DISCUSSION

**3.1. Morphology and Structural Properties of AuNP Catalysts.** In this work, we employed commercially available Au/TiO<sub>2</sub>, Au/Al<sub>2</sub>O<sub>3</sub>, and Au/ZnO nanoparticles and mesoporous Au-loaded TiO<sub>2</sub> nanoparticle assemblies (Au/MTA) as catalysts for the reduction of various nitro compounds. All commercial catalysts have a Au loading of 1 wt % and possess an average gold crystallite size of ~2–3 nm. To prepare the mesoporous Au/MTA(*x*) with various loadings of gold (*x* = 0.5, 1, and 2 wt %), a surfactant-assisted aggregated assembly of titanium compounds [Ti(OPr)<sub>4</sub> and TiCl<sub>4</sub>] was used. Gold nanoparticles were deposited by the deposition–precipitation method.<sup>13</sup> The products obtained after cautious removal of the surfactants consist of a continuous network of tightly interconnected gold and anatase TiO<sub>2</sub> nanoparticles and exhibit a large internal surface area (approximately 110–120 m<sup>2</sup> g<sup>–1</sup>) and a narrow pore size distribution (approximately 7.5–7.6 nm), according to the small-angle X-ray scattering (SAXS), transmission electron microscopy (TEM), and N<sub>2</sub> physisorption measurements; these results are reported elsewhere (Figure S1 of the Supporting Information).<sup>13</sup> On the basis of TEM analysis, we found that the average Au particle size is strongly related to the gold loading as determined by elemental microprobe analysis (EDS) and continuously increased from 3.2 to 4.4 nm and from 4.4 to 5.2 nm while the gold loading was increased from 0.5 to 1% and from 1 to 2%, respectively

[named Au/MTA(0.5), Au/MTA(1), and Au/MTA(2), respectively (Table T1 of the Supporting Information)]. The average size of titania particles estimated using the Guinier approximation on the low- $q$  range of X-ray scattering data was found to be  $\sim 10$  nm.

**3.2. Evaluation of the Catalytic Reactions.** To optimize the reaction conditions, the reduction of 4-nitro toluene (**1**) using different hydrides, solvents, and supported gold catalysts was initially investigated (Table 1). Specifically, the supported

**Table 1. Evaluation of Supported Au Catalysts, Hydride Compounds, and Solvents in the Catalytic Reduction of 4-Nitrotoluene (**1**) into 4-Toluidine (**1a**)**

entry	catalyst <sup>a</sup>	solvent	hydrogen source (equiv) <sup>b</sup>	time (h)/yield (%) <sup>c</sup>
1	Au/TiO <sub>2</sub>	DCM	NaBH <sub>4</sub> (6)	2/5
2	Au/TiO <sub>2</sub>	THF	NaBH <sub>4</sub> (6)	2/43
3	Au/TiO <sub>2</sub>	EtOAc	NaBH <sub>4</sub> (6)	2/4
4	Au/TiO <sub>2</sub>	CH <sub>3</sub> CN	NaBH <sub>4</sub> (6)	2/41
5	Au/TiO <sub>2</sub>	MeOH	NaBH <sub>4</sub> (6)	1/96
6	Au/TiO <sub>2</sub>	EtOH	NaBH <sub>4</sub> (6)	1/>99 (97) <sup>d</sup>
7	Au/TiO <sub>2</sub>	EtOH	NaBH <sub>4</sub> (4)	4/52
8	no catalyst	EtOH	NaBH <sub>4</sub> (4)	4/no reaction
9	Au/TiO <sub>2</sub>	EtOH	NaH (20)	4/no reaction <sup>e</sup>
10	Au/TiO <sub>2</sub>	EtOH	LiBH <sub>4</sub> (6)	4/no reaction <sup>e</sup>
11	Au/TiO <sub>2</sub>	EtOH	BH <sub>3</sub> ·THF (6)	4/no reaction <sup>e</sup>
12	Au/MTA(0.5)	EtOH	NaBH <sub>4</sub> (6)	1/49
13	Au/MTA(1)	EtOH	NaBH <sub>4</sub> (6)	1/98
14	Au/MTA(2)	EtOH	NaBH <sub>4</sub> (6)	1/>99 (98) <sup>d</sup>

<sup>a</sup>Twenty milligrams of each catalyst was used (1 mol %). <sup>b</sup>Hydride fold excess of millimoles based on starting material. <sup>c</sup>Relative yield of **1a** determined by <sup>1</sup>H NMR. <sup>d</sup>Values in parentheses correspond to the isolated yield. <sup>e</sup>THF (dry) was also used as a solvent.

gold catalyst (1 wt % in Au) was placed in a 5 mL glass reactor, followed by the addition of ethanol (1 mL), substrate (0.1 mmol), and hydride compound, and the reaction mixture was vigorously stirred for the appropriate time. To our delight, Au/TiO<sub>2</sub> in the presence of NaBH<sub>4</sub> and ethanol as solvent provide fast, quantitative, and clean reduction without the requirement of any chromatographic purification of product **1a** (Table 1, entry 6). The amount of NaBH<sub>4</sub> (4–6-fold molar excess, based on the nitroarene concentration) used in our experiments is significantly smaller than that in previous studies employing similar reductions; they used a 50–650-fold molar excess of NaBH<sub>4</sub>.<sup>9</sup> Therefore, our protocol is highly appealing for practical applications. In addition, after completion of **1**, as evidenced by thin layer chromatography (TLC), the slurry was filtered through a short pad of Celite and silica to withhold the catalyst with the aid of ethanol or methanol ( $\sim 5$  mL). Then, the filtrate was evaporated under reduced pressure to give pure 4-toluidine **1a** (97% yield) as a brown solid. It is worth noting that in the presence of NaH, LiBH<sub>4</sub>, or BH<sub>3</sub>·THF hydrides, no conversion of nitro compound **1** was observed (Table 1, entries 9–11). Even if THF was used as a reaction solvent, no reduction product was observed after prolonged reaction times (results not shown). In addition, Au/Al<sub>2</sub>O<sub>3</sub> was found to catalyze the reduction of **1** to **1a** in good yield (91% yield, 1 h), while Au/ZnO is a less efficient catalyst (5% yield, 1 h) (see

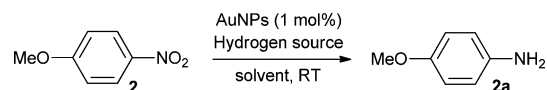
Figure S2 of the Supporting Information). To elucidate if the protic solvent is necessary for this catalytic process, the reduction of **1** also occurred in EtOAc, THF, and CH<sub>3</sub>CN upon addition of small amounts of water (5, 9, and 18  $\mu$ L). A substantial enhancement of the nitroarene consumption was observed in the presence of 18  $\mu$ L (1 mmol) of water, forming the corresponding aniline **1a** in good to high yields (Figure S3 of the Supporting Information). This result suggests that a protic solvent is necessary for the efficient reduction of nitroarenes under the reaction conditions described above, by means of a possible protonation process of the nitro group and/or the possible enhancement of the borohydride reagent solubility; even further mechanistic studies are required.

To compare the catalytic activity of Au/TiO<sub>2</sub> with that of mesoporous Au/MTA assemblies, we studied the reduction of **1** with Au/MTA( $x$ ) ( $x = 0.5, 1, \text{ and } 2$ ) catalysts in the presence of NaBH<sub>4</sub> and ethanol as solvents. For the purpose of comparison, we also prepared Au/TiO<sub>2</sub> (P25) catalyst by precipitating 2 wt % gold on Degussa P25 ( $\sim 26$  nm particle size,  $53 \text{ m}^2 \text{ g}^{-1}$ ) nanoparticles and evaluated their catalytic performance under similar reaction conditions (Figure S2 of the Supporting Information). The evolution of the hydrogenation products (Table 1, entries 12–14) indicated that Au/MTA( $x$ ) materials, although they afforded excellent selectivity (>99%) of **1**, in 1 h, possess moderate-to-high yield (approximately 49–99%) to the corresponding amine (**1a**), which is highly related to the Au loading amount and particle size. Among them, the Au-MTA(2) catalyst associated with 5 nm AuNPs showed the best catalytic activity in terms of conversion (Table T1 of the Supporting Information). Of particular note was the fact that **1** was completely reduced by Au/MTA(2) within 1 h, yielding **1a** as the only product; no detectable amounts of azoxy- and azobenzene derivatives were observed in the reaction mixture based on NMR spectroscopy. These findings are in good agreement with previous studies, which suggest that gold particles in the range of 3–5 nm are more active for Ar-NO<sub>2</sub> reduction.<sup>13</sup> Control experiments showed no obvious transformation of **1** in the absence of catalyst or in the presence of gold-free TiO<sub>2</sub> (MTA) support, confirming that gold particles are essential for hydrogenation reactions.

To determine if the examined catalysts might also be applicable for the chemoselective reduction of nitro compounds in the presence of different hydrogen donor molecules, such as dimethylphenylhydrosilane (DMPS), triethylhydrosilane (TES), and 1,1,3,3-tetramethyldisiloxane (TMDS), we performed the reduction of 4-nitroanisole (**2**) catalyzed by Au/TiO<sub>2</sub> and Au/MTA(2). All the reactions were conducted in a 5 mL glass reactor at ambient temperature, using a variety of organic solvents. As shown in Table 2, the reduction occurs faster over both catalysts in ethanol and THF with 2.5 equiv of TMDS, giving the corresponding amine **2a** in >98% yield in up to 30 min (Table 2, entries 2, 8, and 9). Even in water, the reduction of **2** proceeds fast enough to afford **2a** in 42% yield, as determined by <sup>1</sup>H NMR (after aqueous phase extraction with ethyl acetate). To the best of our knowledge, only one study that examined the reduction of nitroarenes in the presence of hydrosilanes using magnetically separable gold nanoparticles Au/Fe<sub>3</sub>O<sub>4</sub> as catalyst appeared recently in the literature,<sup>10</sup> even longer reaction times were required.

**3.3. Chemoselective Reduction of Nitro Compounds with NaBH<sub>4</sub> or TMDS Catalyzed by Mesoporous Au/MTA Assemblies.** To study the limitation of this practical

**Table 2. Evaluation of Hydrosilanes and Solvents in the Reduction of 4-Nitroanisole (2) into 4-Anisidine (2a) Catalyzed by Au/TiO<sub>2</sub> or Au/MTA(2)**



entry	catalyst <sup>a</sup>	solvent	hydrogen source (equiv) <sup>b</sup>	yield (%) <sup>c</sup>
1	Au/TiO <sub>2</sub>	DCM	TMDS (2.5)	64
2	Au/TiO <sub>2</sub>	THF	TMDS (2.5)	98
3	Au/TiO <sub>2</sub>	EtOAc	TMDS (2.5)	60
4	Au/TiO <sub>2</sub>	CH <sub>3</sub> CN	TMDS (2.5)	67
5	Au/TiO <sub>2</sub>	toluene	TMDS (2.5)	66
6	Au/TiO <sub>2</sub>	MeOH	TMDS (2.5)	97
7	Au/TiO <sub>2</sub>	H <sub>2</sub> O	TMDS (2.5)	42
8	Au/TiO <sub>2</sub>	EtOH	TMDS (2.5)	>99
9	Au/MTA(2)	EtOH	TMDS (2.5)	>99
10	no catalyst	EtOH	TMDS (2.5)	no reaction
11	Au/MTA(2)	EtOH	TMDS (2)	90
12	Au/MTA(2)	EtOH	PDMS (5)	94
13	Au/MTA(2)	EtOH	TES (5)	85

<sup>a</sup>With regard to catalysts, 20 mg of each catalyst was used (1 mol %).

<sup>b</sup>Hydrosilane fold excess in millimoles based on starting material.

<sup>c</sup>Yields of 2a as determined by <sup>1</sup>H NMR after 30 min.

chemoselective reduction process, a series of nitroarenes (3–18) were examined (Table 3), under the conditions described above. Notably, Au/TiO<sub>2</sub> and Au/MTA(2) gave similar activities (see Tables 1 and 2); the latter was used for these catalytic reductions, using NaBH<sub>4</sub> and TMDS (values in parentheses) as the hydrogen donor molecules. In all cases, the corresponding substituted anilines were formed, with excellent yields (>90%) and selectivity (>99%). Inert-atmosphere conditions are preferable, as under open air, minor amounts of azoxyarenes can be occasionally seen via a gold-catalyzed aerobic oxidation of the produced anilines.<sup>17</sup> As shown in Table 3, among the two reducing agents, TMDS affords faster reaction rates (the reactions were complete in up to 1 h), judging from the TLC analysis.

As seen in Table 3, *p*-dinitrobenzene (4) was completely reduced to the corresponding diamine (4a) in 1 h in 94% isolated yield using NaBH<sub>4</sub> and in 98% yield in 0.5 h using TMDS. Chloro- and bromo-substituted nitroarenes (5 and 6, respectively) were also reduced without undergoing any dehalogenation (Table 3, entries 3 and 4, respectively). Also, carboxylic, carboxylate, and cyano functionalities in 8, 9, and 13 nitroarenes remain intact under these conditions, indicating highly chemoselective reduction. However, in the case of carbonyl-substituted nitroarenes, such as 4-nitroacetophenone (10) and 4-nitrobenzaldehyde (11), the corresponding hydroxyl aryl amines [10b and 11b, respectively (see the Supporting Information)] were isolated as the only product when NaBH<sub>4</sub> was used as the reducing agent. On the other hand, the presence of TMDS (2.5 equiv) does not affect the carbonyl groups of the nitroarenes, giving the corresponding carbonyl-substituted anilines (10a and 11a) as the only products (Table 3, entries 8 and 9, respectively). In the reduction of 15, the benzyl-protected moiety remains intact, under the reaction conditions presented here (Table 3, entry 13), using either NaBH<sub>4</sub> or TMDS as the reducing agent. Also, the reduction of 6-nitro-1*H*-indazole (16) and 6-nitroisobenzofuran-1(3*H*)-one (17) gave the corresponding amines

**Table 3. Chemoselective Reduction of Nitro Compounds (8–18) with NaBH<sub>4</sub> and TMDS Catalyzed by Mesoporous Au/MTA(2) Material<sup>a</sup>**

Entry	Reactant	Product	NaBH <sub>4</sub> (TMDS) <sup>b</sup>	Time(h)/Yield(%)
1			4	3 / 95
2			6 (5)	1 / 94 (0.5 / 98)
3			5 (2.5)	1 / 97 (0.5 / 98)
4			5	1 / 92
5			5 (2.5)	3 / 90 (0.5 / 94)
6			6 (2.5)	3 / 95 (1 / 92)
7			5 (2.5)	1 / 94 (0.5 / 93)
8			5 (2.5)	1 / 97 <sup>c</sup> (0.3 / 98)
9			5 (2.5)	1 / 98 <sup>c</sup> (0.3 / 97)
10			5 (2.5)	3 / 92 (0.5 / 95)
11			5	1 / 92
12			4	3 / 93
13			4 (2.5)	3 / 95 (0.5 / 97)
14			6	8 / 90
15			6 (2.5)	6 / 94 (1 / 96)
16			(2.5)	(0.3 / 98)

<sup>a</sup>Twenty milligrams of Au/MTA(2) was used (1 mol %). <sup>b</sup>Hydride fold excess on a molar basis of the starting material. <sup>c</sup>The corresponding hydroxyl aryl amines 10b and 11b were formed (see the Supporting Information). The values in parentheses correspond to the times/yields of the reduction in the presence of TMDS.

without further transformation of the pyrazole and lactone rings. These results clearly support the high chemoselectivity of the present Au/MTA-NaBH<sub>4</sub> and Au/MTA-TMDS catalytic systems, with the latter being the more efficient one.

Because of the extended network of interconnected gold and TiO<sub>2</sub> nanoparticles, the Au/MTA(2) catalyst can be easily separated from the reaction mixture by simple filtration and can be reused for the next catalytic run. The stability of the Au/MTA was examined in repeated catalytic experiments. As

shown in Figure S4 of the Supporting Information, the catalyst can be used at least six times without a significant loss of its catalytic activity and selectivity.

To further probe the feasibility of the present catalytic systems in a small-scale synthesis, 3-nitrostyrene (**18**) was reduced under the experimental conditions described above using Au/MTA(2) catalyst and TMDS as the hydrogen donor molecule (Table 3, entry 16). In this case, 3-aminostyrene (**18a**) was observed as the only product, through the formation of the corresponding unsaturated hydroxylamine **18b** (Figure S16 of the Supporting Information). Because no reduction of the C=C bond was observed, the high chemoselectivity of the catalyst by means of preferential hydrogen transfer reduction can be inferred. Unlike in the case of TMDS, in the presence of NaBH<sub>4</sub>, further reduction of the C=C double bond was observed by <sup>1</sup>H NMR. On the basis of the high chemoselectivities, and the fast and clean reaction processes, we propose that the Au/MTA(2)-TMDS catalytic system can be used for various hydrogenation reactions, including amine synthesis.

It is interesting to note here that reduction of 1-nitroalkanes **19** and **20** gave the corresponding azoalkanes (**19d** and **20d**, respectively) as the only products, in the presence of a 10-fold molar excess of NaBH<sub>4</sub> or a 5-fold molar excess of TMDS, within 180 and 20 min, respectively (Figure 1). However, after

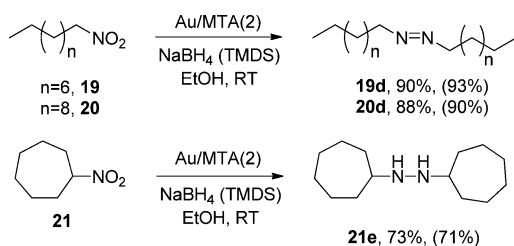


**Figure 1.** Reduction of nitroalkanes (**19**–**21**) with NaBH<sub>4</sub> and TMDS (values in parentheses) catalyzed by mesoporous Au/MTA(2) material.

a prolonged reaction time (12 h), the corresponding hydrazo compounds were observed in significant amounts, accompanied by a small amount of alkyl amines **19a** and **20a** (results not shown). On the other hand, nitro cycloheptane (**21**) transformed into the corresponding hydrazo compound **21e** (Figure 1). Similar results were obtained when NaBH<sub>4</sub> was used as the reducing agent, although a prolonged reaction time is required.<sup>18</sup> These results are in contrast with previous studies that report on the reduction of nitro compounds with Au/TiO<sub>2</sub> and hydrazine hydrate. In that case, the corresponding alkyl amines were observed as the only products.<sup>11</sup>

**3.4. Mechanistic Studies.** To rationalize a possible mechanistic pathway for the present gold-catalyzed reduction of nitroarenes, we investigated the primary kinetic isotope effects (KIEs) of the reduction of 4-chloronitrobenzene (**5**) using NaBH<sub>4</sub> and NaBD<sub>4</sub> as reducing agents. In general, KIEs are a powerful tool for probing the transition state (TS) and provide valuable information about the extent of bond breaking and bond making of a reaction.<sup>19</sup> We also report here a Hammett-type kinetic study for the reduction of a diverse set of para-X-substituted nitroarenes and discuss the mechanistic possibilities.

The KIEs were determined by monitoring the consumption of **5** ( $x$ ) in the presence of NaBH<sub>4</sub> or NaBD<sub>4</sub> using <sup>1</sup>H NMR.

For this reason, 0.2 mmol of **5**, 1 mol % Au/MTA(2), and 0.2 mmol of NaBH<sub>4</sub> (or NaBD<sub>4</sub>) were stirred in ethanol (1 mL), and a 100  $\mu$ L aliquot of the mixture was taken at 0.5, 1.5, 3, and 5 min time intervals. The mixture was filtered through a short pad of Celite and silica (to withhold the catalyst) and washed with ethanol (~1 mL). Then the filtrate was evaporated under reduced pressure, and the corresponding consumptions of **5** were determined by integrating the appropriate proton signals in <sup>1</sup>H NMR spectra. Each reaction was repeated at least five times, and the average values are depicted in Figures S5–S7 of the Supporting Information.

On the basis of this analysis, a plot of  $\ln(x)$  versus time yielded a straight line with a slope equal to a pseudo-first-order reaction rate constant ( $k$ ), eq 1. Assuming that the rate constant of the reduction using NaBH<sub>4</sub> is equal to  $k_H$ , while that obtained using NaBD<sub>4</sub> is  $k_D$ , a  $k_H/k_D$  ratio of  $1.60 \pm 0.05$  is determined, which is proportional to the primary KIE (Figure S7 of the Supporting Information). The substantial primary isotope effects found here suggest that B–H(D) bond cleavage occurs in a slow step, while at a same time a [Au]–H(D) bond is formed.<sup>20</sup> A substantial KIE was also measured in a previous hydrogenation study, suggesting dissociation of H<sub>2</sub> (vs D<sub>2</sub>) on a gold surface is the rate-determining step in a bimetallic Au@Pt/TiO<sub>2</sub> system-catalyzed hydrogenation of nitro aromatic compounds.<sup>4d</sup> A similar KIE ( $k_H/k_D = 1.54$ ) was observed in the transfer hydrogenation of nitroarenes in the presence of CO/H<sub>2</sub>O<sup>6b</sup> upon switching the solvent from H<sub>2</sub>O to D<sub>2</sub>O; however, this observation does not necessarily provide solid evidence with regard to the rate-determining step of the reduction. To evaluate the influence of the heterogeneous nature of the catalyst in the measurement of KIEs, we performed the same kinetics using Au/Al<sub>2</sub>O<sub>3</sub> and Au/TiO<sub>2</sub> (commercially available). Similar values for both kinetics were measured:  $k_H/k_D = 1.79$ , and  $k_H/k_D = 1.71$ , respectively (Figures S5 and S6 of the Supporting Information, respectively). This result indicates that the heterogeneous support of the catalyst plays an insignificant role in the transition state of the reduction process. Therefore, we propose that the *in situ*-formed gold hydrides ([Au]–H) are responsible for the reduction of nitroarenes.

After KIE studies, a formal kinetic analysis of a series of X-substituted nitroarenes [X = MeO (**2**), H (**3**), Cl (**5**), COOMe (**9**), and CN (**13**)] was performed (Figure 2). Considering that the concentration of gold hydride species remains constant at initial times ( $t < 3$  min) and assuming a pseudo-first-order dependence of the reaction rate on the nitroarene concentration, eq 1 can be applied.

$$\ln(x) = -kt \quad (1)$$

where  $k$  is the rate constant and  $x$  is the consumption of the X-substituted nitroarene at reaction time  $t$ .

According to eq 1, a plot of  $\ln(x)$  versus time should provide a linear curve with a slope equal to the rate constant  $kx$ . It is worth noting that the kinetic activity of **2**, **3**, **5**, **9**, and **13** nitroarenes is remarkably affected by the nature of the X substituent group, in which the reduction proceeds faster as the electron-withdrawing ability of the substituent group improves. For example, the reduction of **9**, **13**, and **5** (4-COOMe, 3-CN, and 4-Cl, respectively) proceeds faster than the corresponding reduction of nitrobenzene **3** (X = H) (Figure 2) in the presence of either NaBH<sub>4</sub> or TMDS, as indicated by the relative rate constant ratios (Figures S8 and S9 of the Supporting Information). On the other hand, nitroarene **2** (MeO-)

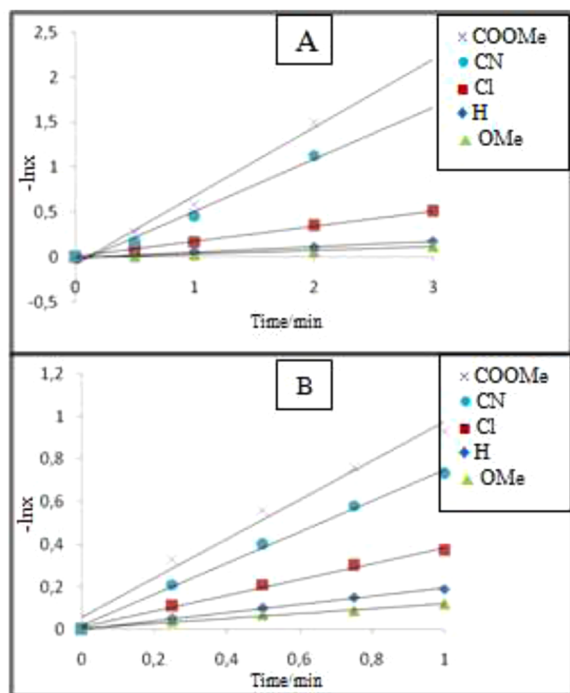


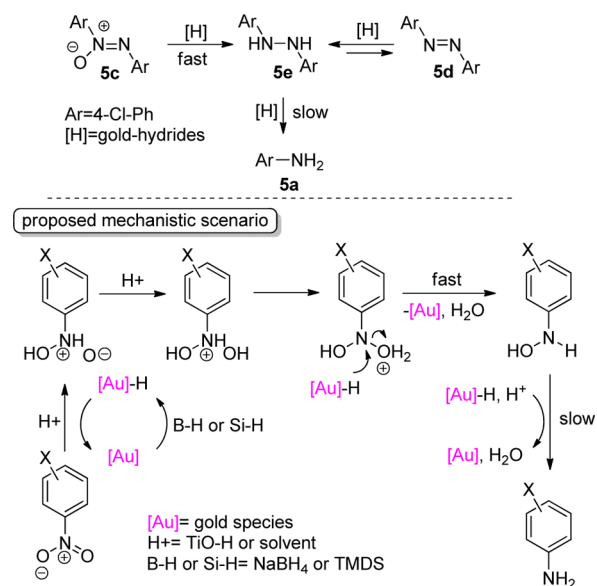
**Figure 2.** Kinetic analysis of the Au/MTA(2)-catalyzed reduction of para-*X*-substituted nitroarenes [*X* = MeO (2), H (3), Cl (5), COOMe (9), and CN (13)] using NaBH<sub>4</sub> (A) and TMDS (B). The reductions with TMDS occurred at 0 °C.

containing an electron-donating group was reduced with a slower reaction rate (Figure 2);  $k_{\text{H}}/k_{\text{MeO}} = 0.7\text{--}0.6$  as determined using NaBH<sub>4</sub> and TMDS. In addition to these results, a Hammett-type correlation in the competition of para-*X*-substituted nitroarenes [*X* = CH<sub>3</sub>O (2), Cl (5), and COOMe (9)] versus nitrobenzene (3), for the reductions with NaBH<sub>4</sub> and TMDS, gave positive slopes:  $\rho \approx 0.55$ , and  $R^2 = 0.9997$  (using  $\sigma^+$  values);  $\rho \approx 0.95$ , and  $R^2 = 0.9989$  (using  $\sigma$  values) (Figures S10 and S11 of the Supporting Information). These results indicate the development of a negative charge (or hydride transfer) in the transition state, which is better stabilized by electron-withdrawing substituents.

It is worth noting that, using an equimolar amount of NaBH<sub>4</sub> (based on millimoles of nitroarene), hydroxylamines **2a**, **3a**, **5b**, **9a**, and **13b** were formed as the major products, even after a prolonged reaction time (1 h), in CD<sub>3</sub>OD as the reaction solvent (Figures S12–S15 of the Supporting Information). The evolution of the reaction was monitored by NMR spectroscopy directly after filtration of the reaction mixture through a small pad of Celite and silica. In these reactions, 0.2 mmol of nitroarenes, 1 mol % Au/MTA(2), and 0.2 mmol of NaBH<sub>4</sub> (or 0.3 mmol of TMDS) were stirred in CD<sub>3</sub>OD (1 mL), and a 100  $\mu\text{L}$  aliquot of the mixture was taken at appropriate time intervals. No significant amount of the corresponding azoxy-, azo-, or hydrazobenzenes was detected by <sup>1</sup>H NMR spectroscopy. In addition, under our experimental conditions,

azoxyarene (**5c**) is reduced to the corresponding hydroazoarene (**5d**) within 1 h, while after a prolonged reaction time (6 h), **5d** is transformed into the corresponding azo compound (**5e**) via a possible gold-catalyzed aerobic oxidation process (Scheme 1).<sup>15</sup>

### Scheme 1. Proposed Mechanism for the Reduction of Nitroarenes Using NaBH<sub>4</sub> or TMDS Catalyzed by Gold Nanoparticles



Also, 4-chloronitrosobenzene was also reduced under the same reaction conditions, giving a mixture of amine **5a** and hydroazoarene **5e**, at 30 min, with the former as the major product.

According to the observations described above, we propose a general mechanistic pathway for the AuNP-catalyzed reduction of nitroarenes. First, a B–H (or Si–H) bond cleavage occurs in a rate-determining step to give the [Au]–H species (Scheme 1).<sup>20</sup> Such species are responsible for the rapid reduction of nitroarenes into the corresponding hydroxylamines, a mechanistic pathway that does not follow the classical direct route (nitroarene → nitrosoarene → aryl hydroxylamine → aniline) but possibly skips the nitrosoarene intermediate. This pathway found support from the KIE studies in which a significant normal primary isotope effect was observed. Also, catalytic experiments conducted in CD<sub>3</sub>OD suggested the formation of the corresponding hydroxylamines as the only intermediate products. The presence of water (protonation pathway) seems to play a crucial role in the reaction rate, while the nature of the heterogeneous support plays an insignificant role under our reaction conditions. On the basis of the kinetic profiles, nitroarenes bearing electron-withdrawing substituents were reduced faster than those with electron-donating groups, results that found support from the Hammett-type kinetic analysis ( $\rho \approx 0.55$ , and  $\rho \approx 0.95$ ). Finally, hydroxylamines are reduced under the conditions described here in a second slow step into the corresponding amines.

## 4. CONCLUSIONS

Herein, we report a detailed study of the reduction of nitroarenes into the corresponding amines, catalyzed by AuNPs loaded on mesoporous TiO<sub>2</sub> (Au/MTA). On the basis of product analysis, nitroarenes are cleanly reduced to the

corresponding anilines in the presence of  $\text{NaBH}_4$  or TMDS in moderate to high yields. Under similar conditions, nitroalkanes are reduced to the corresponding diazo and hydrazone compounds. According to the substantial measured kinetic isotope effects (KIEs), B–H(D) bond cleavage and [Au]–H(D) bond formation have been suggested to occur in a rate-determining step. Gold hydrides are responsible for the reduction of nitroarenes into the corresponding aryl amines, through the formation of hydroxylamines as the only or major intermediate. Hammett-type kinetics supports the observation of a negative charge in the transition state of the reaction. On the basis of the high chemoselectivities and the fast and clean reaction processes, both catalytic systems Au/MTA- $\text{NaBH}_4$  and Au/MTA-TMDS can be used for various hydrogenation reactions, including fine synthesis of amine.

## ■ ASSOCIATED CONTENT

### Supporting Information

Kinetic profiles of the reductions, Hammett-type kinetics,  $^1\text{H}$  and  $^{13}\text{C}$  NMR data, and NMR spectra of the amines and hydroxylamines. This material is available free of charge via the Internet at <http://pubs.acs.org>.

## ■ AUTHOR INFORMATION

### Corresponding Author

\*Telephone: +30-2310-997871. Fax: +30-2310-997679. E-mail: [lykakis@chem.auth.gr](mailto:lykakis@chem.auth.gr).

### Notes

The authors declare no competing financial interest.

## ■ ACKNOWLEDGMENTS

Financial support by the European Union and the Greek Ministry of Education (ERC-09, MESOPOROUS-NPs, and ARISTEIA-2691) and the Aristotle University of Thessaloniki Research Committee (KA 89309) is kindly acknowledged. We thank Dr. E. Evgenidou for obtaining the LC–MS data.

## ■ REFERENCES

- (1) Lawrence, S. A. *Amines: Synthesis, Properties and Applications*; Cambridge University Press: New York, 2004.
- (2) Blaser, H.-U.; Steine, H.; Studer, M. *ChemCatChem* **2009**, *1*, 210.
- (3) (a) Mitsudome, T.; Kaneda, K. *Green Chem.* **2013**, *15*, 2636. (b) Stratakis, M.; Garcia, H. *Chem. Rev.* **2012**, *112*, 4469. (c) Zhang, Y.; Cui, X.; Shi, F.; Deng, Y. *Chem. Rev.* **2012**, *112*, 2467. (d) Corma, A.; Garcia, H. *Chem. Soc. Rev.* **2008**, *37*, 2096. (e) Takale, B.; Bao, M.; Yamamoto, Y. *Org. Biomol. Chem.* **2014**, *12*, 2005.
- (4) (a) Corma, A.; Serna, P. *Science* **2006**, *313*, 332. (b) Corma, A.; Concepcion, P.; Serna, P. *Angew. Chem., Int. Ed.* **2007**, *46*, 7266. (c) Boronat, M.; Concepcion, P.; Corma, A.; Gonzalez, S.; Illas, F.; Serna, P. *J. Am. Chem. Soc.* **2007**, *129*, 16230. (d) Serna, P.; Concepcion, P.; Corma, A. *J. Catal.* **2009**, *265*, 19.
- (5) (a) Chen, Y. Y.; Qiu, J. S.; Wang, X. K.; Xiu, J. H. *J. Catal.* **2006**, *242*, 227. (b) He, D. P.; Shi, H.; Wu, Y.; Xu, B. Q. *Green Chem.* **2007**, *9*, 849. (c) Liu, L.; Qiao, B.; Ma, Y.; Zhang, J.; Deng, Y. *Dalton Trans.* **2008**, 2542. (d) Shimizu, K.; Miyamoto, Y.; Kawasaki, T.; Tanji, T.; Tai, Y.; Satsuma, A. *J. Phys. Chem. C* **2009**, *113*, 17803. (e) Cardenas-Lizana, F.; Gomez-Quero, S.; Perret, N.; Keane, M. A. *Catal. Sci. Technol.* **2011**, *1*, 652. (f) Matsushima, Y.; Nishiyabu, R.; Takahashi, N.; Haruta, M.; Kimura, H.; Kubo, Y. *J. Mater. Chem.* **2012**, *22*, 24124. (g) He, D.; Jiao, X.; Jiang, P.; Wang, J.; Xu, B.-Q. *Green Chem.* **2012**, *14*, 111. (h) Kartusch, C.; Makosch, M.; Sa, J.; Hungerbuehler, K.; van Bokhoven, J. A. *ChemCatChem* **2012**, *4*, 236.
- (6) (a) Liu, L.; Qiao, B.; Chen, Z.; Zhang, J.; Deng, Y. *Chem. Commun.* **2009**, 653. (b) He, L.; Wang, L. C.; Sun, H.; Ni, J.; Cao, Y.; He, H.-Y.; Fan, K.-N. *Angew. Chem., Int. Ed.* **2009**, *48*, 9538.

(c) Huang, J.; Yu, L.; He, L.; Liu, Y.-M.; Cao, Y.; Fan, K.-N. *Green Chem.* **2011**, *13*, 2672.

(7) Lou, X. B.; He, L.; Qian, Y.; Liu, Y. M.; Cao, Y.; Fan, K.-N. *Adv. Synth. Catal.* **2011**, *353*, 281.

(8) (a) Liu, X.; Ye, S.; Li, H.-Q.; Liu, Y.-M.; Cao, Y.; Fan, K.-N. *Catal. Sci. Technol.* **2013**, *3*, 3200. (b) Tang, C.-H.; He, L.; Liu, Y.-M.; Cao, Y.; He, H.-Y.; Fan, K.-N. *Chem.—Eur. J.* **2011**, *17*, 7172. (c) Peng, Q.; Zhang, Y.; Shi, F.; Deng, Y. *Chem. Commun.* **2011**, *47*, 6476. (d) Xiang, Y.; Meng, Q.; Li, X.; Wang, J. *Chem. Commun.* **2010**, *46*, 5918.

(9) (a) Shin, H. S.; Huh, S. *ACS Appl. Mater. Interfaces* **2012**, *4*, 6324. (b) Zhang, F.; Liu, N.; Zhao, P.; Sun, J.; Wang, P.; Ding, W.; Liu, J.; Jin, J.; Ma, J. *Appl. Surf. Sci.* **2012**, *263*, 471. (c) Dotzauer, D. M.; Bhattacharjee, S.; Wen, Y.; Bruening, M. L. *Langmuir* **2009**, *25*, 1865. (d) Tan, X.; Zhang, Z.; Xiao, Z.; Xu, Q.; Liang, C.; Wang, X. *Catal. Lett.* **2012**, *142*, 788. (e) Hayakawa, K.; Yoshimura, T.; Esumi, K. *Langmuir* **2003**, *19*, 5517. (f) Kuroda, K.; Ishida, T.; Haruta, M. *J. Mol. Catal. A: Chem.* **2009**, *298*, 7. (g) Jiang, H. L.; Akita, T.; Ishida, T.; Haruta, M.; Xu, Q. *J. Am. Chem. Soc.* **2011**, *133*, 1304. (h) Liu, W.; Yang, X.; Huang, W. *J. Colloid Interface Sci.* **2006**, *304*, 160. (i) Yan, N.; Zhang, J.; Yuan, Y.; Chen, G. T.; Dyson, P. J.; Li, Z. C.; Kou, Y. *Chem. Commun.* **2010**, *46*, 1631. (j) Wu, S.; Dzubiella, J.; Kaiser, J.; Drechsler, M.; Guo, X.; Ballauff, M.; Lu, Y. *Angew. Chem., Int. Ed.* **2012**, *51*, 2229. (k) Wei, H.; Lu, Y. *Chem.—Asian J.* **2012**, *7*, 680. (l) Wu, F.; Yang, Q. *Nano Res.* **2011**, *4*, 861. (m) Praharaj, S.; Nath, S.; Ghosh, S. K.; Kundu, S.; Pal, T. *Langmuir* **2004**, *20*, 9889. (n) Tang, R.; Liao, X. P.; Shi, B. *Chem. Lett.* **2008**, 834. (o) Wang, Y.; Wei, G.; Wen, F.; Zhang, X.; Zhang, W.; Shi, L. *J. Mol. Catal. A: Chem.* **2008**, *280*, 1. (p) Lee, J.; Park, J. C.; Song, H. *Adv. Mater.* **2008**, *20*, 1523. (q) Yao, Y.; Sun, Y.; Han, Y.; Yan, C. *Chin. J. Chem.* **2010**, *28*, 705. (r) Qiu, L.; Peng, Y.; Liu, B.; Lin, B.; Peng, Y.; Malik, M. J.; Yan, F. *Appl. Catal., A* **2012**, *413*, 230. (s) Esumi, K.; Miyamoto, K.; Yoshimura, T. *J. Colloid Interface Sci.* **2002**, *254*, 402. (t) Wang, X.; Liu, D.; Song, S.; Zhang, H. *Catal. Sci. Technol.* **2012**, *2*, 488. (u) Layek, K.; Kantam, M. L.; Shirai, M.; Hamane, D. N.; Sasaki, T.; Maheswaran, H. *Green Chem.* **2012**, *14*, 3164.

(10) Park, S.; Lee, I. S.; Park, J. *Org. Biomol. Chem.* **2013**, *11*, 395.

(11) Gkizis, P. L.; Stratakis, M.; Lykakis, I. N. *Catal. Commun.* **2013**, *36*, 48.

(12) Vasilikiogiannaki, E.; Gryparis, C.; Kotzabasaki, V.; Lykakis, I. N.; Stratakis, M. *Adv. Synth. Catal.* **2013**, *355*, 907.

(13) Tamiolakis, I.; Fountoulaki, S.; Vordos, N.; Lykakis, I. N.; Armatas, G. S. *J. Mater. Chem. A* **2013**, *1*, 14311.

(14) Recent selected examples: (a) Gryparis, C.; Efe, C.; Raptis, C.; Lykakis, I. N.; Stratakis, M. *Org. Lett.* **2012**, *14*, 2956. (b) Lykakis, I. N.; Psyllaki, A.; Stratakis, M. *J. Am. Chem. Soc.* **2011**, *133*, 10426. (c) Efe, C.; Lykakis, I. N.; Stratakis, M. *Chem. Commun.* **2011**, *47*, 803. (d) Kotzabasaki, V.; Lykakis, I. N.; Gryparis, C.; Psyllaki, A.; Vasilikiogiannaki, E.; Stratakis, M. *Organometallics* **2013**, *32*, 665.

(15) Gilbert, K. E.; Borden, W. T. *J. Org. Chem.* **1979**, *44*, 659.

(16) Tamiolakis, I.; Lykakis, I. N.; Katsoulidis, A. P.; Armatas, G. S. *Chem. Commun.* **2012**, *48*, 6687.

(17) Grirrane, A.; Corma, A.; Garcia, H. *Science* **2008**, *322*, 1661.

(18) Rahaim, R. J.; Maleczka, R. E. *Org. Lett.* **2005**, *7*, 5087.

(19) (a) Carpenter, B. K. *Determination of Organic Reaction Mechanisms*; John Wiley & Sons: New York, 1984. (b) Melander, L.; Saunders, W. H. *Reactions Rates of Isotopic Molecules*; John Wiley & Sons: New York, 1980. (c) Matsson, O.; Westaway, K. C. *Adv. Phys. Org. Chem.* **1996**, *31*, 143–248.

(20) (a) Conte, M.; Miyamura, H.; Kobayashi, S.; Chechik, V. *J. Am. Chem. Soc.* **2009**, *131*, 7189. (b) Abad, A.; Almela, C.; Corma, A.; Garcia, H. *Chem. Commun.* **2006**, 3178. Selected examples for stable gold hydride complexes: (c) Lehner, H.; Matt, D.; Pregosin, P. S.; Venanzi, L. M. *J. Am. Chem. Soc.* **1982**, *104*, 6825. (d) Wang, X.; Andrews, L. *Angew. Chem., Int. Ed.* **2003**, *42*, 5201. (e) Rosca, D. A.; Smith, D. A.; Hughes, D. L.; Bochmann, M. *Angew. Chem., Int. Ed.* **2012**, *51*, 10643. (f) Grirrane, A.; Garcia, H.; Corma, A.; Alvarez, E. *Chem.—Eur. J.* **2013**, *19*, 12239. (g) Yan, M.; Jin, T.; Ishikawa, Y.; Minato, T.; Fujita, T.; Chen, L.-Y.; Bao, M.; Asao, N.; Chen, M.-W.;

Yamamoto, Y. *J. Am. Chem. Soc.* **2012**, *134*, 17536. (h) Yan, M.; Jin, T.; Chen, Q.; Ho, H. E.; Fujita, T.; Chen, L.-Y.; Bao, M.; Chen, M.-W.; Asao, N.; Yamamoto, Y. *Org. Lett.* **2013**, *15*, 1484. (i) Takale, B. S.; Tao, S. M.; Yu, X. Q.; Feng, X. J.; Jin, T.; Bao, M.; Yamamoto, Y. *Org. Lett.* **2014**, *16*, 2558.